

Amphiphilic Janus Micelles with Polystyrene and Poly(methacrylic acid) Hemispheres

Rainer Erhardt,[†] Mingfu Zhang,[†] Alexander Böker,^{†,‡} Heiko Zettl,[‡] Clarissa Abetz,[§] Peter Frederik,^{||} Georg Krausch,^{‡,⊥} Volker Abetz,^{*,†} and Axel H. E. Müller^{*,†,⊥}

Contribution from the Makromolekulare Chemie II, Physikalische Chemie II, Bayreuther Institut für Makromolekülforschung, and Bayreuther Zentrum für Kolloide und Grenzflächen, Universität Bayreuth, D-95440 Bayreuth, Germany, and EM-unit, University Maastricht, Post-box 616, NL-6200 MD Maastricht, The Netherlands

Received October 16, 2002; E-mail: volker.abetz@uni-bayreuth.de; axel.mueller@uni-bayreuth.de

Abstract: We describe the synthesis and the solution properties of Janus micelles containing a polybutadiene (PB) core and a compartmentalized corona consisting of a poly(methacrylic acid) (PMAA) and a polystyrene (PS) hemisphere. The Janus micelles were obtained via cross-linking the middle block of a microphase-separated PS-*block*-PB-*block*-PMMA triblock copolymer in the bulk state, followed by alkaline hydrolysis of the poly(methyl methacrylate) (PMMA) ester groups. Results of fluorescence correlation spectroscopy, field flow fractionation, light scattering, cryogenic transmission electron microscopy, scanning electron microscopy, and scanning force microscopy indicate that above a critical aggregation concentration of about 0.03 g/L spherical supermicelles are formed from about 30 PS-PMAA micelles in aqueous solution in the presence of NaCl. These supermicelles have radii of 40–60 nm, significantly increasing on ionization (pH > 6). In addition, very large spherical objects are observed with radii of 100–250 nm.

Introduction

In recent years, the controlled synthesis of complex nanoparticles has attracted increasing interest for both academic and technological reasons. Micellar structures formed from amphiphilic molecules such as block copolymers play an important role in this area. In contact with a selective solvent, amphiphilic block copolymers spontaneously aggregate into micelles, where the less soluble block is forming a core surrounded by chains of the more soluble block, which extend into the solvent phase. An interesting alternative to these centrosymmetric structures are noncentrosymmetric micelles, in which a single core is surrounded by a compartmentalized corona, so-called *Janus micelles*. Due to their inherent asymmetry, these micelles have the potential of aggregating in a higher level of hierarchy. Recently, the synthesis of such structures was described^{1,2} and their solution and surface properties were studied.^{1–3} In short, a linear polystyrene-*block*-polybutadiene-*block*-poly(methyl methacrylate) (PS-PB-PMMA) triblock copolymer was prepared in the bulk state, in which the PB minority block formed spherical microdomains located at the interfaces of a PS-PMMA lamellar

microdomain structure. After the spherical PB microdomains were cross-linked in the ordered bulk state, the material was redissolved in a common solvent. The resulting structures in solution exhibit a PB core surrounded by a compartmentalized corona, half of which consists of PS chains, while the other consists of PMMA chains. These Janus micelles were found to aggregate into larger entities with a very sharp size distribution. Such *supermicelles* coexist with single Janus micelles (*unimers*).¹ Alternatively, micelles or vesicles have also been cross-linked in solution;^{4,5} however, nothing has been reported on the formation of Janus structures.

Here we present the synthesis and characterization of truly amphiphilic Janus micelles with a hydrophobic hemicorona, made of polystyrene (PS), and a hydrophilic hemicorona, made of poly(methacrylic acid) (PMAA), surrounding a cross-linked polybutadiene (PB) core. Using chromatographic, scattering, and imaging techniques, we show that these Janus micelles form spherical supermicelles in addition to even larger spherical entities.

Experimental Section

Synthesis. The synthesis of the precursor PS-PB-PMMA Janus micelles was reported elsewhere.¹ They consist of a polybutadiene (PB) core surrounded by about 13 chains each of PS (DP = 800) and PMMA (DP = 700), which are phase-separated.

The PS-PB-PMMA Janus micelles were dissolved in 1,4-dioxane (ca. 10 wt %) under argon in a sealed high-pressure Schlenk tube, and the PMMA ester groups were hydrolyzed by KOH (molar ratio 3/1)

* To whom correspondence should be addressed. Fax: +49-921-553393.

[†] Makromolekulare Chemie II, Universität Bayreuth.

[‡] Physikalische Chemie II, Universität Bayreuth.

[§] Bayreuther Institut für Makromolekülforschung, Universität Bayreuth.

^{||} University Maastricht.

[⊥] Bayreuther Zentrum für Kolloide und Grenzflächen, Universität Bayreuth.

(1) Erhardt, R.; Böker, A.; Zettl, H.; Kaya, H.; Pyckhout-Hintzen, W.; Krausch, G.; Abetz, V.; Müller, A. H. E. *Macromolecules* **2001**, *34*, 1069.

(2) Saito, R.; Fujita, A.; Ichimura, A.; Ishizu, K. *J. Polym. Sci., Polym. Chem. Ed.* **2000**, *38*, 2091.

(3) Xu, H.; Erhardt, R.; Abetz, V.; Müller, A. H. E.; Goedel, E. A. *Langmuir* **2001**, *17*, 6787–6793.

(4) Thurmond, K. B., II; Huang, H.; Clark, C. G., Jr.; Kowalewski, T.; Wooley, K. L. *Colloids Surf. B* **1999**, *16*, 45.

(5) Stewart, S.; Liu, G. *Angew. Chem.* **2000**, *112*, 348.

using 18-crown-6 as a phase transfer catalyst (molar ratio [18-crown-6]/[MMA unit] = 1/5). The reaction was carried out at 110 °C for 5 days. Finally the solution was further diluted with 1,4-dioxane, precipitated into 1 M hydrochloric acid, and washed with water, before it was dried under vacuum (maximum 50 °C).

Solutions of the obtained PS-PB-PMAA Janus micelles were prepared as follows. Since a direct dissolution in water is not possible (as the PS arms are too long), 0.2 g of a sample was first dissolved in 100 mL of a mixture of 1,4-dioxane and methanol (80:20, v:v). Then, methanol was exchanged by dioxane/water (80:20, v:v) via dialysis using dialysis tubes from regenerated cellulose (Medicell, 12–14 kDa), and afterwards 1,4-dioxane was stepwise replaced by water via dialysis. Finally the solution was dialyzed against pure water (MilliQ) three times, to get rid of the last traces of 1,4-dioxane. Aqueous solutions containing 1 wt % NaCl were finally obtained by two dialysis steps of the aqueous polymer solutions against a solution of 1 wt % NaCl in water. The salt was added to avoid the stretching of the partially dissociated PMAA blocks ("polyelectrolyte effect"). The last dialysate was used to dilute this primary solution in order to obtain lower concentrations.

Characterization. IR spectroscopy was performed using a Bruker FTIR Equinox 55/S spectrometer at a resolution of 4 cm⁻¹. The sample was prepared from a solution cast on a Ge disk.

Fluorescence correlation spectroscopy (FCS) was carried out on a Zeiss ConfoCor 2 spectrometer, using the single photon count mode for the avalanche photodiode. Cresyl violet (Lamda Physics, $\lambda_{\text{exc}} = 575$ nm, $\lambda_{\text{emiss}} = 620$ nm) was used as a dye at a concentration of 10⁻⁹ mol/L. The diffusion coefficients and the hydrodynamic radii of the dye-carrying particles were calculated on the basis of the waist radius of the laser beam. The diffusion coefficients and the hydrodynamic radii were calculated on the basis of the beam waist radius ($r_w = 200$ nm) determined from measurements of Rhodamin 6G. The FCS experiments were performed days after preparation of the solutions, and they were repeated after 2 weeks.

Static light scattering (SLS) was performed on a Sofica SLS goniometer 1 using a He-Ne laser ($\lambda = 632.8$ nm) at 25 °C. The refractive index increment ($dn/dc = 0.170$ at $\lambda = 632.8$ nm) was determined using the PSS NFT ScanRef scanning interferometer against the dialysate.⁶

Dynamic light scattering (DLS) measurements were performed on an ALV-SP 125 goniometer using a ALV 5000 correlator and a He-Ne laser. Sample preparation was similar to the static light scattering experiments.

Asymmetric flow field-flow fractionation (AF-FFF) was accomplished on a Postnova HRFFF-10000 system equipped with RI, UV, and multiangle light scattering (Wyatt DAWN EOS, $\lambda = 632.8$ nm) detectors: dimension of the channel, 0.35 mm; cutoff molecular weight of the membrane, 5000; injection volume, 100 μ L; cross-flow gradient, 79.5–0% within 30 min, followed by a laminar flow for 10 min; laminar flow out, 1 mL/min; eluent, water with 1 wt % NaCl; sample concentration, 1.323 g/L.

Cryogenic transmission electron microscopy (cryo-TEM) was performed on a Philips CM 12 at 120 kV in low-dose mode. Sample droplets on a carbon-coated Cu grid were automatically blotted several times in an atmosphere saturated with water vapor and then vitrified in liquid ethane by using a Vitrobot from Maastricht Instruments (patent licensed to FEI for worldwide distribution). The sample was then transferred to the cryo-TEM (Gatan 626 cryoholder and cryo-transfer system) and imaged at about -170 °C.

Scanning electron microscopy (SEM) was performed on a LEO 1530 field emission microscope using secondary electron detection. The samples were obtained by applying a drop of a salt-free aqueous

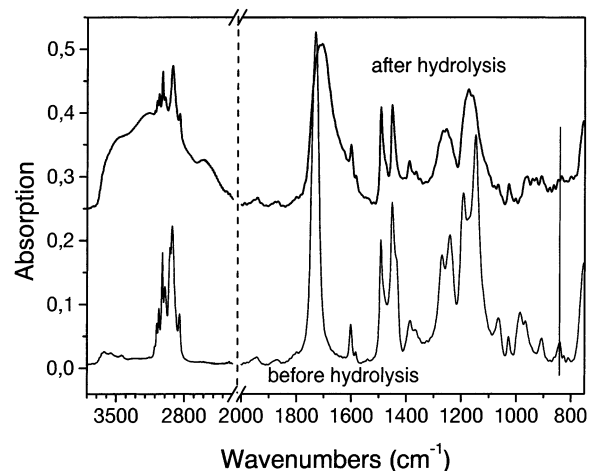


Figure 1. FTIR spectra before and after hydrolysis. The line at 841 cm⁻¹ indicates the position of a characteristic vibration of the methyl ester.

solution ($c = 0.2$ g/L, pH 3.7) onto a silicon wafer followed by drying at room temperature or onto a silicon wafer at a temperature of 100 °C.

Scanning force microscopy (SFM) images were taken on a Digital Instruments Dimension 3100 microscope operated in the tapping mode (free amplitude of the cantilever ~ 20 nm, set point ratio ~ 0.98). The samples were obtained by applying a drop of a salt-free aqueous solution ($c = 0.2$ g/L, pH 3.7) onto a silicon wafer followed by drying.

Results and Discussion

The PMMA blocks of the cross-linked PS-PB-PMMA Janus micelles were hydrolyzed in order to obtain Janus micelles with a hydrophobic PS hemisphere and a polyelectrolyte PMAA hemisphere.

Infrared Spectroscopy (IR). The result of the hydrolysis under alkaline conditions is shown in Figure 1. At 841 cm⁻¹ there is a typical vibration band from the methyl ester group (symmetrical vibration of the C–C–O–C entity),⁷ the intensity of which is significantly decreased after hydrolysis (see the solid vertical line in Figure 1). After hydrolysis, two additional vibrational transitions typical of the hydrolyzed product are observed at 849 and 835 cm⁻¹, respectively. Furthermore, there is a characteristic shift of the C=O valence vibration from 1731 cm⁻¹ (ester) to 1706 cm⁻¹ (acid), and there are typical broad bands of the OH valence vibration of the acid between 3700 and 2400 cm⁻¹. At 2600 cm⁻¹ the O–H stretching vibration of carbonic acid dimers can be observed.⁸ From the IR results the degree of hydrolysis can be estimated to be >90%.

Fluorescence Correlation Spectroscopy (FCS). Figure 2A shows a set of FCS autocorrelation functions $G(t)$ taken at different concentrations of Janus micelles in aqueous solution containing 0.17 M NaCl. Below a polymer concentration of some 0.03 ± 0.02 g/L the experimentally determined $G(t)$ can be modeled by a single species of molecularly dissolved cresyl violet molecules. At higher polymer concentrations, $G(t)$ changes in a characteristic way. First, we observe a faster decay at short correlation times, which is characteristic of an increased fraction of triplet losses, indicative of a change in the chemical environment of the dye molecules. In addition, $G(t)$ develops two shoulders at around 1–10 ms (region I in Figure 2A) and around 100–1000 ms (region II in Figure 2A). These two

(6) Becker, A.; Köhler, W.; Müller, B. *Ber. Bunsen-Ges. Phys. Chem.* **1995**, *99*, 600.

(7) Smith, P.; Goulet, L. *J. Polym. Sci., Polym. Phys. Ed.* **1993**, *31*, 327.

(8) Ogura, K.; Sobue, H. *Polym. J.* **1972**, *3*, 153.

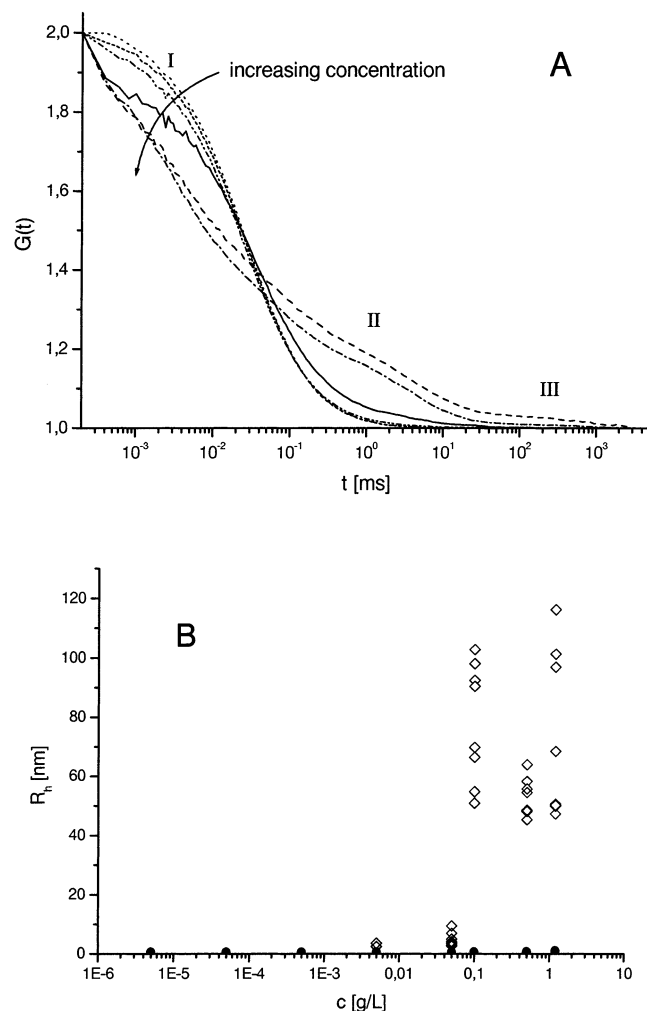


Figure 2. (A) FCS autocorrelation functions of PS-PB-PMAA Janus micelles in water (plus 0.17 M NaCl) at polymer concentrations of (—) 1.2, (- · - ·) 0.5, (—) 0.1, (- · · -) 0.05, (- - -) 0.005, and (····) 0.0005 g/L. (B) Hydrodynamic radii obtained from the experimental data in (A) by least-squares fits assuming a single species (for $c < 0.01$ g/L) and two species (for $c > 0.01$ g/L), respectively. The critical aggregation concentration (cac) was determined as the concentration at which, in addition to the free dye molecules, also the particles are observed in solution (cac $\approx 0.03 \pm 0.02$ g/L).

shoulders are indicative of small fractions of dye molecules moving considerably slower than the majority. In other words, we observe fractions of larger particles. The first shoulder can be reproduced by a fit to the data, assuming two fractions of particles with different hydrodynamic radii. In contrast, the second shoulder is difficult to model, as no well-defined experimental value for $G(t \rightarrow \infty)$ is available. Therefore, we have modeled the data at higher polymer concentrations by two fractions, one corresponding to isolated dye molecules (filled circles in Figure 2B) and the second corresponding to dye molecules incorporated into an aggregate of Janus micelles (open diamonds in Figure 2B). We may therefore locate a critical aggregation concentration (cac) between 0.01 and 0.1 g/L, above which molecularly dissolved Janus micelles (unimers) aggregate to polymolecular supermicelles (multimers). The hydrodynamic radius of these aggregates lies in the range $\langle R_h \rangle_n = 54 \pm 6$ nm. We already reported a similar observation for PS-PB-PMMA Janus micelles in nonselective organic solvents.¹ In addition to the supermicelles, species with a much larger hydrodynamic radius (several hundred nanometers to micrometers) seem to

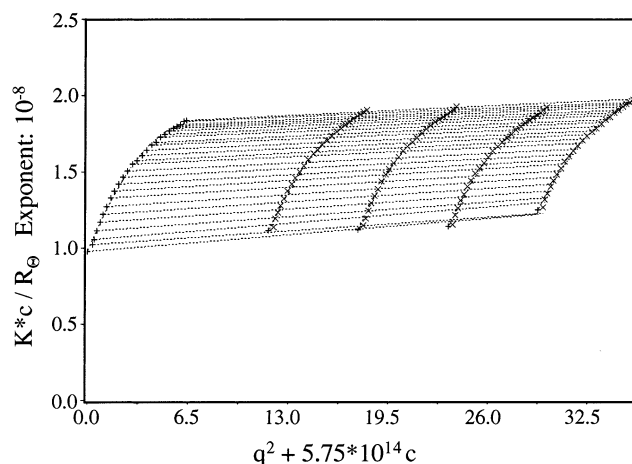


Figure 3. Zimm plot of the PS-PB-PMAA Janus micelles in water plus 0.17 M NaCl ($0.1 \leq c \leq 0.5$ g/L).

exist, although at a very low concentration. The FCS experiments, however, do not allow us to draw conclusions about the dynamics of the aggregate formation, since it is known that frozen micelles also exhibit a cmc (or cac)^{9,10} and low-molecular-weight fluorescence dye may also diffuse into frozen micelles.

Static Light Scattering (SLS). To get more information about the molecular weight and the size of the aggregates, light scattering measurements were performed. Figure 3 shows a Zimm plot of the results of aqueous Janus micelle solutions containing 0.17 M NaCl. From the Zimm plot a weight-average molecular weight of $M_w = 1.02 \times 10^8$ g/mol and a z-average radius of gyration, $R_g = 87$ nm, are obtained. In the case of block copolymers with different refractive indices of the blocks the values for R_g and M_w determined by SLS are apparent ones and are usually different from their true values. However, it has been shown that the chemical heterogeneity of aggregates (micelles) which consist of a number of unimers is much smaller than the heterogeneity of the unimers. In this case SLS yields the true R_g and M_w values, respectively.^{11–13} The second virial coefficient is positive ($A_2 = 2.43 \times 10^{-6}$ mol mL/g). Assuming complete hydrolysis of the PMMA arms and 13 precursor triblock copolymer chains per Janus micelle, its total weight-average molecular weight should be around 2.1×10^6 g/mol. The weight-average molecular weight obtained by light scattering thus corresponds to a species composed of about 48 unimeric Janus micelles.

We note that the curvature of the angular dependence of the scattered intensity in the Zimm plot may have different reasons. Cylindrically shaped (rodlike) structures could lead to such a curvature. However, in view of the results obtained by cryo-TEM (see below), we anticipate that the high polydispersity of the samples causes the observed curvature.¹⁴ A high polydispersity may result from the coexistence of various species of different sizes (unimers, supermicelles, and larger aggregates).

- (9) Procházka, K.; Kiserow, D.; Ramireddy, C.; Tuzar, Z.; Munk, P.; Webber, S. E. *Macromolecules* **1992**, *25*, 454.
- (10) Tian, M.; Qin, A.; Ramireddy, C.; Webber, S. E.; Munk, P.; Tuzar, Z.; Procházka, K. *Langmuir* **1993**, *9*, 1741.
- (11) Quin, A.; Tian, M.; Ramireddy, C.; Webber, S. E.; Munk, P.; Tuzar, Z. *Macromolecules* **1994**, *27*, 120.
- (12) Webber, S. E.; Munk, P.; Tuzar, Z. *Macromolecules* **1994**, *27*, 120.
- (13) Vorlicek, J.; Kratochvil, P. *J. Polym. Sci., Polym. Phys. Ed.* **1973**, *11*, 1251.
- (14) *Classical Light Scattering from Polymer Solutions*; Kratochvil, P., Ed.; Elsevier: Amsterdam, 1987.

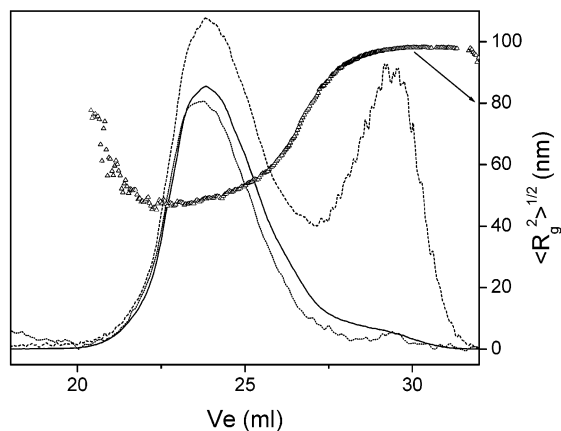


Figure 4. AF-FFF-MALS measurements of Janus micelles in water with 0.17 M NaCl: (—) LS 90°; (---) LS 35°; (···) RI; (Δ) radius of gyration.

Asymmetric Flow Field-Flow Fractionation (AF-FFF). The existence of the different micellar species in aqueous solution was also proven by AF-FFF with an MALS detector (Figure 4). The AF-FFF eluogram clearly shows two distinguishable species separated by the cross-flow, especially at low scattering angles. The very strong angular dependence for the second species indicates its large size, whereas its amount is so small that it is almost invisible in the concentration signal (RI). By application of the Debye method (and light scattering data fitting with a polynomial of second order) the z -average root-mean-square radii of gyration of two species were determined to be $R_g = 63$ and 118 nm, respectively. The z -average R_g value of the whole sample is 78.2 nm, which is quite close to the result obtained from static light scattering. Due to the huge sizes of the micellar species and small cutoff molecular weight of the membrane used for the measurement, the sample loss during the measurement should be negligible. Assuming 100% mass recovery, the first peak corresponds to a weight-average molecular weight of $M_w = 7.8 \times 10^7$ g/mol (and a number of 37 Janus micelles per particle). The concentration signal of the second peak was too noisy to allow molecular weight determination.

Dynamic Light Scattering (DLS). DLS was performed on samples in different solutions (1,4-dioxane/methanol, 1,4-dioxane/water). In Figure 5 we show the hydrodynamic radii as a function of solvent composition. Replacement of methanol by water leads to a slight increase of the hydrodynamic radius, which further increases upon increasing the water concentration. This may be attributed to an increasing degree of dissociation of the acid groups in the PMAA blocks. In the absence of organic solvent the hydrodynamic radius is increased by about a factor of about 2 compared to what is found in a 80/20 1,4-dioxane/water mixture. In pure water, the addition of salt causes a reduction of the aggregate size back to the value found in 80/20 1,4-dioxane/methanol mixtures. This reduction can be attributed to the screening of the repulsive forces within the charged chains, which in turn leads to a reduced chain stretching. An example for the results of the CONTIN analysis used for the determination of the hydrodynamic radii is shown in Figure 6 (for a sample obtained after dialysis). Besides the peak related to the supermicelles, also a very small peak is observed which corresponds either to unimers or to very small amounts of residual cleavage product (not visible in GPC) which may have

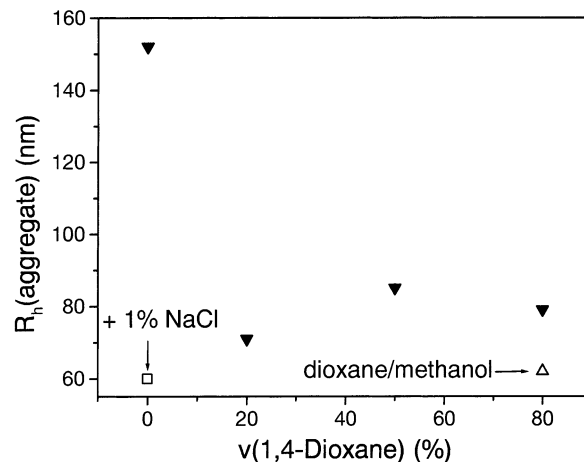


Figure 5. Hydrodynamic radii of the supermicelles as a function of solvent composition (1,4-dioxane/water) during dialysis of the PS-PMAA Janus micelles.

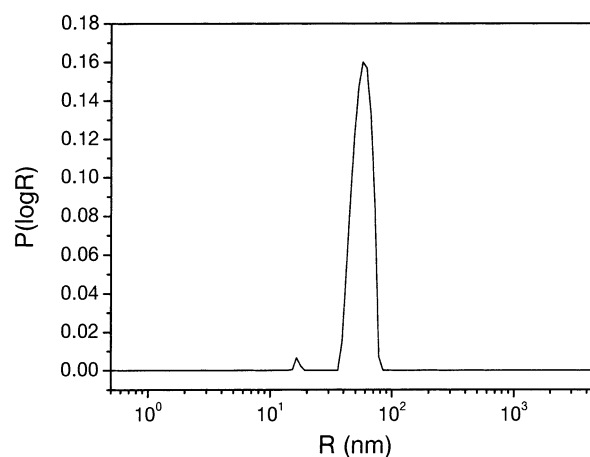


Figure 6. Distribution function of the radii of the PS-PMAA Janus micelles in water plus 0.17 M NaCl (from CONTIN analysis of the autocorrelation function $g_2(t) - 1$; $c = 1.32$ g/L; $\theta = 90^\circ$).

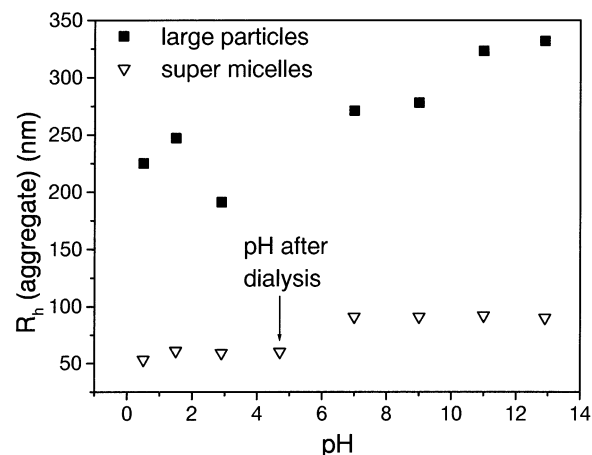


Figure 7. pH dependence of the hydrodynamic radii of aggregates of Janus micelles in water (plus 0.17 M NaCl).

resulted from the synthesis strategy for the PS-PB-PMMA Janus micelles (radical cross-linking in bulk).

In aqueous solutions containing 0.17 M NaCl the hydrodynamic radius of the supermicelles slightly shrinks with decreasing pH (Figure 7). This finding may be attributed to the reduced degree of dissociation. (The pH was controlled by the addition of NaOH and HCl solutions.) Accordingly, with increasing pH

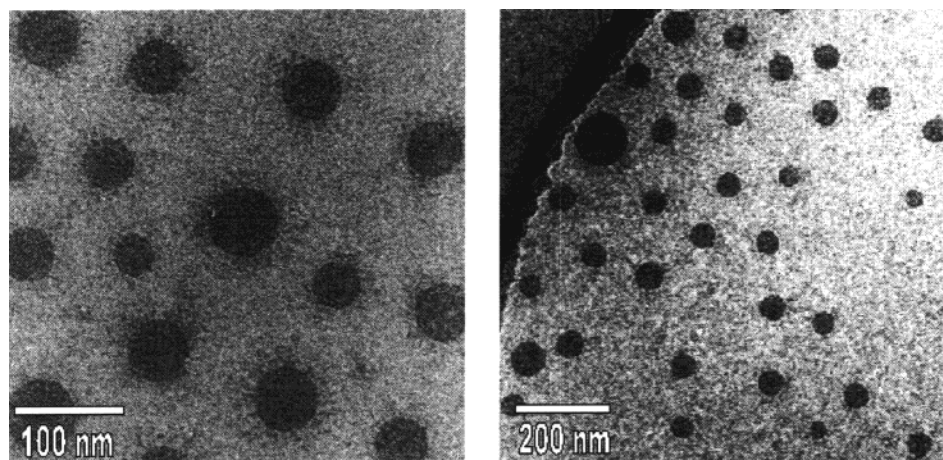


Figure 8. Cryo-TEM micrographs of the Janus micelle aggregates in water plus 0.17 M NaCl.

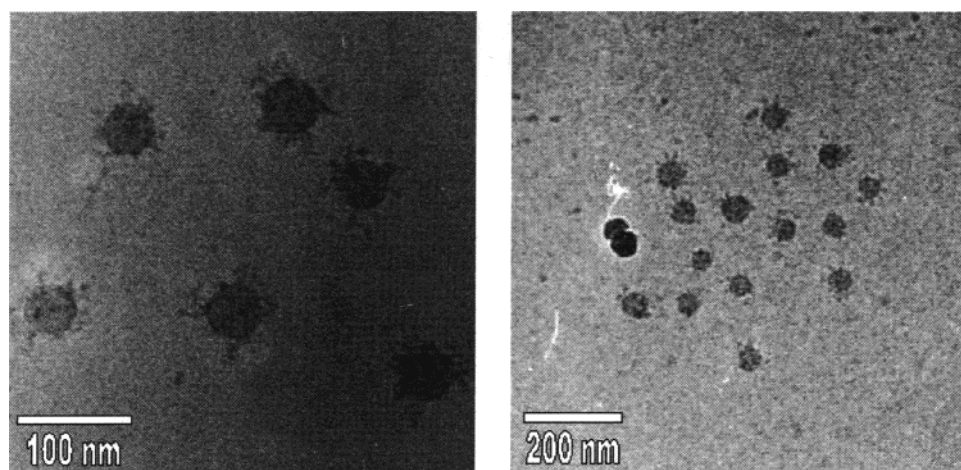


Figure 9. Cryo-TEM micrographs of the Janus micelle aggregates in pure water.

the size of the aggregates increases, because the higher degree of dissociation leads to a stretching of the PMAA arms. The increase mainly occurs at $4.6 < \text{pH} < 7$: i.e., the range where ionization of PMAA occurs.¹⁵ In addition to the supermicelles, also a very small number of larger particles are observed in the CONTIN analysis, having hydrodynamic radii between 190 and 330 nm for lower and higher pH values (although their existence at the pH value after dialysis is suspected to be due to a broadening of the CONTIN peak). The dependence of their size on pH is qualitatively similar to that of the supermicelles.

Cryogenic Transmission Electron Microscopy (cryo-TEM). To visualize the aggregates in solution, cryo-TEM was performed on solutions in pure water and in aqueous solutions containing 0.17 M NaCl. These measurements were performed without additional staining or etching. Figure 8 shows spherical objects in the vitrified matrix. Around the dark spheres a slightly shaded corona can be detected. While the dark cores can be assigned to the hydrophobic components (PS and PB), the diffuse corona may be assigned to the PMAA arms, which are not aggregated and have a weaker contrast to water. It can also be seen that the particles are not uniform in size, but there also exist larger particles. Statistical analysis of a larger number of cryo-TEM images yields a fraction of 0.6% large particles among the total number of particles. The smaller particles have

a core diameter of 24.6 ± 3.6 nm (number-average value obtained from 30 smaller particles). Including the highly swollen corona, this would roughly correspond to a radius of 45–55 nm for the whole particle, which again compares reasonably well to the hydrodynamic radius obtained by DLS. The larger particles observed by cryo-TEM have radii in the range of 60 nm, and no further particles with much larger sizes were observed. This is due to the sample preparation, which limits the size of observable particles to the thickness of the sample layer. Particles in the micrometer size, as indicated by FCS, may not be observable by cryo-TEM. When the supermicelles are studied in salt-free aqueous solution, the cores of the supermicelles look the same. However, the corona chains appear to aggregate into a few strands (Rasta hair like, Figure 9), an effect which to our knowledge has not been reported in the literature before. Assigning the total core area to the PS and PB blocks and using the PS bulk density of 1.052 g/cm^3 , we can estimate the total number-average molecular weight of these supermicelles as $M_n = 6.5 \times 10^7 \text{ g/mol}$. Together with the number of 800 styrene and 180 butadiene repeating units per precursor block copolymer and the association number of 13 block copolymer chains per Janus micelle (from the primary bulk structure before cross-linking), an association number of 28 ± 10 Janus micelles per supermicelle is calculated.

Scanning Electron Microscopy (SEM). SEM was performed without staining at low acceleration voltage ($<1 \text{ kV}$) on a

(15) Dautzenberg, H.; Jaeger, W.; Kötzt, J.; Philipp, B.; Seidel, C.; Stscherbina, D. *Polyelectrolytes*; Carl Hanser Verlag: München, 1994.

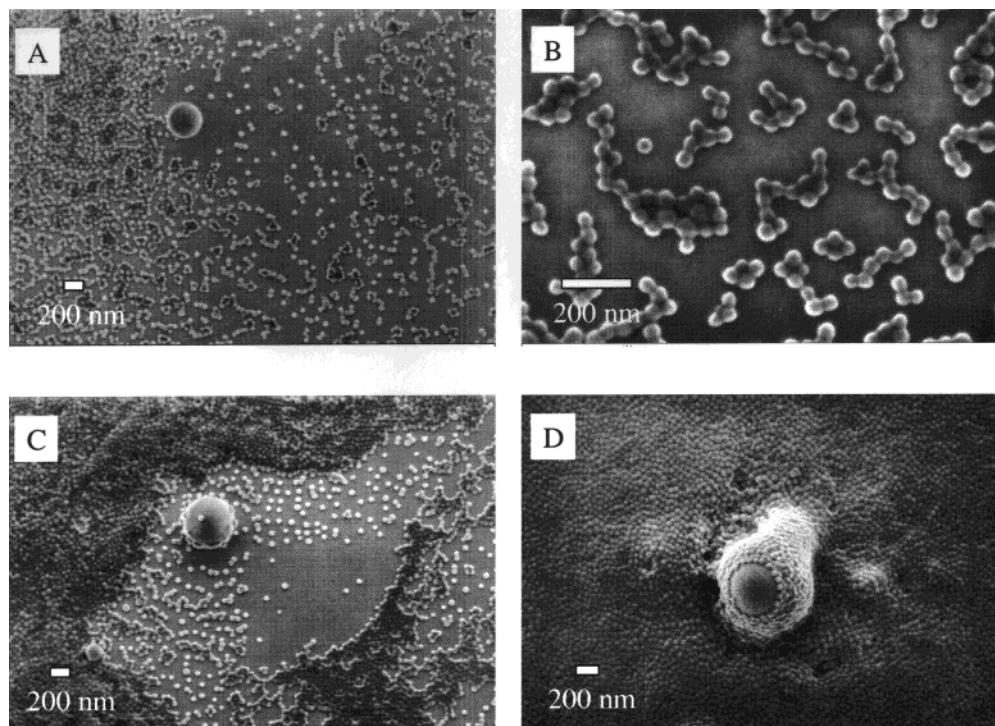


Figure 10. SEM micrographs of the Janus micelle aggregates on a Si wafer prepared from pure water at room temperature (A, B) and at 100 °C (C, D).

sample obtained by drying a droplet of the salt-free solution on a silicon wafer at room temperature. Parts A and B of Figure 10 show a large number of small spheres which can be assigned to the supermicelles ($R \approx 25$ nm; we note that the apparent size of the supermicelles determined by electron microscopy may be somewhat smaller than expected due to possible beam damage of the PMAA blocks). In addition, also a small number of very large spherical objects with diameters between ca. 100 and 250 nm are observed, which are covered in part by the supermicelles (Figure 10A). When the droplet is dried on a hot silicon wafer (100 °C), the supermicelles aggregate rapidly and form multilayers (Figure 10C,D). The larger spherical objects in these multilayer areas appear to be more covered than in other areas. Thus, we think that the coverage by supermicelles is most likely due to the drying process, since the huge objects can be found in the whole range from “naked” to “completely covered”. The nature of the huge objects is unclear. They might be agglomerates of supermicelles or multilamellar vesicles. This question will be discussed below.

Scanning Force Microscopy (SFM). Finally, we investigate the morphological properties of the supermicelles by SFM after drying a droplet of a dilute salt-free aqueous solution on a silicon wafer. Figure 11 shows topography (parts A, C, and E) and phase images (parts B, D, and F). We observe hemispherical objects (see cross-section in Figure 11G) which seem to locally aggregate in a two-dimensional, loosely packed way. This aggregation may be caused by capillary forces during the drying process. Both the radius and height of these objects are in the range 44 ± 5 nm, which is on the same order of magnitude as the value obtained by FCS for the hydrodynamic radius in solution. Especially in Figure 11D also smaller particles can be observed in addition to supermicelles. The size of the small particles is more difficult to determine unambiguously, as their radius ($R = 5\text{--}10$ nm) is of about the same size as the tip radius. We may assign them to single PS-PB-PMAA Janus micelles.

Such unimers could not be observed by cryo-TEM, most likely due to their low concentration. They may, however, accumulate in thin films on a solid substrate due to favorable interactions between the PMAA hemisphere and the polar SiO_x surface layer. This finding is in agreement with the CONTIN analysis discussed above, which also indicated the presence of a smaller species in solution.

The supermicelles formed by PS-PB-PMMA Janus micelles prior to hydrolysis showed a different, “fried egg” structure on silicon. This structure was attributed to the adsorption of PMMA to the silicon, while PS formed a droplike domain on top. This notion implies that the superstructure formed in THF solution was transformed by the preferential wetting of one of the outer blocks. In the case of the supermicelles from PS-PB-PMAA, however, such a breakup of the superstructure does not seem to occur. In contrast to the case before hydrolysis, the PS compartment of the aggregates is expected to be glassy in a nonsolvent such as water. Therefore, significant rearrangements of the chains in contact with a surface are not to be expected. The spherical supermicelles appear to be deformed to hemispheres when being adsorbed from an aqueous solution onto silicon. This may simply be due to the collapse of the PMAA chains on drying.

As seen before in SEM, besides the supermicelles, also a smaller number of very large spherical objects are observed which appear to have a substructure (parts E and F of Figure 11).

Conclusions

We have been able to synthesize truly amphiphilic Janus micelles consisting of a PB core and a corona made up from two compartments of PS and PMAA, respectively. In aqueous solution the majority of the PS-PMAA Janus micelles form spherical supermicelles above a critical aggregation concentration of around 0.03 mg/L.

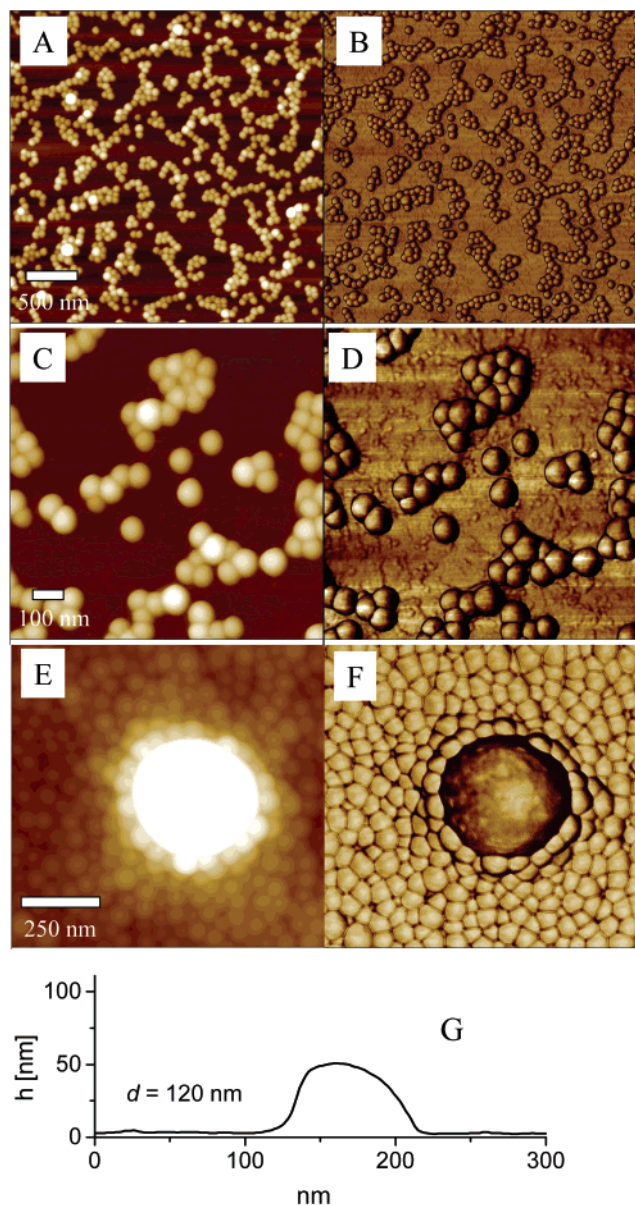
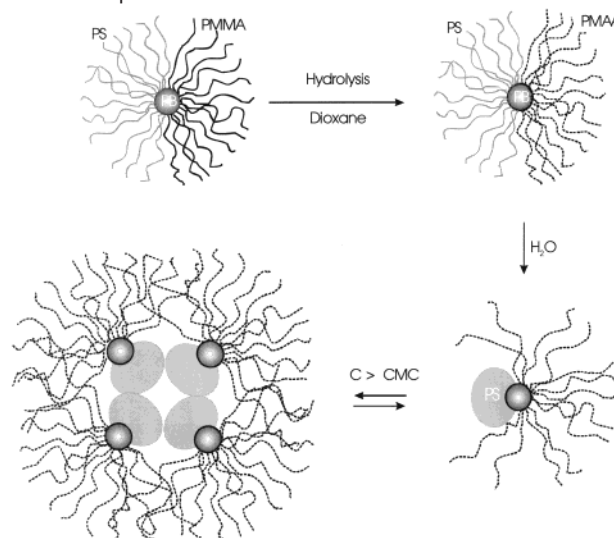


Figure 11. Tapping mode SFM images of Janus micelle aggregates on a Si wafer prepared from pure water: (A, C, E) topography (0–100 nm); (B, D, F) phase (0–25°); (G) cross-section through one of the supermicelles in Figure 11C.

A few questions need to be addressed.

(i) *What is the shape of the single Janus micelles in aqueous solution?* Obviously, the PS hemicorona will be in a collapsed, glassy state. The PMAA arms emanating from the cross-linked PB core will have a tendency to spread over a large volume, especially at $\text{pH} > 5$, when PMAA becomes ionized, leading to a structure similar to a star polymer or frozen star micelle (see Scheme 1). On the other hand, PMAA is incompatible with PS and PB; thus, it will not completely surround the collapsed PS/PB core and we have to assume that at least a partial noncentrosymmetric character remains. Due to their low concentration it is very difficult to design an experiment which returns the structure of the unimers in aqueous solution. High electric fields might possibly stabilize the unimers and at the same time allow SAXS or SANS measurements in the oriented state. X-ray or neutron reflectivity measurements at the water–air or water–oil interface might reveal their structure

Scheme 1. Synthesis and Tentative Structure of Janus Micelles and Their Supermicelles



in the form where one or both hemicoronas are expanded, respectively.

(ii) *What is the structure of the supermicelles?* The spherical shape suggests a PS core and a corona made up of many PMAA hemicoronas. In these supermicelles the hydrophobic PS arms of 20–40 Janus micelles form the collapsed core and the PMAA arms form the solubilizing corona. Thus, the inherently noncentrosymmetric Janus micelles are stabilized by forming a centrosymmetric superstructure. Depending on the preparation of the solution, two scenarios can be discussed for the structure of the core (a) During the dialysis procedure from dioxane/methanol via dioxane/water to pure water unimers form which later aggregate to the supermicelles. In that case the core of the supermicelle will consist of many glassy PS/PB cores and the supermicelle can be assumed to be dynamic. This would also explain why the FCS dye only penetrates the supermicelles (i.e. in the void between PS/PB cores), not the unimers. (b) During the dialysis supermicelles are directly formed. In that case the core of the supermicelle will be glassy and the supermicelle has to be regarded as frozen.

With respect to the cac value, the structure of the core is an important parameter. Unexpectedly, the cac value observed here is about 4 times larger than for the PS-PB-PMMA Janus micelles in THF, a solvent for both hemicoronas. This might indicate that the supermicelle core is, in fact, composed of many frozen unimer cores which easily dissociate. In addition, on dissociation the PMAA arms can expand into a larger volume, thus stabilizing the core.

(iii) *What is the size and aggregation number of the supermicelles?* Table 1 shows the aggregation numbers and radii obtained by the various experimental methods. Taking into account that light scattering renders a weight average and cryo-TEM a number average aggregation number, the agreement of both methods is very good. The SLS data obtained after AF-FFF are more reliable than those obtained from the whole solution, because the small number of huge particles has a strong effect on the weight average. With respect to size, there is a good agreement between AF-FFF/MALS and DLS, both taken at $\text{pH} 5$. The SFM value is a number average rather than a z -average, which explains the lower value. The SEM value

Table 1. Comparison of Aggregation Numbers, N_{agg} , and Supermicelle Sizes Obtained by Different Methods in Water with 0.17 M NaCl

method	N_{agg}	$R_{\text{supermicelles}}$, nm	$R_{\text{giant micelles}}$, nm
FCS		$R_{\text{h}} = 40-100$	
SLS	$\langle N \rangle_{\text{w}} = 48$	$\langle R_{\text{g}} \rangle_{\text{z}} = 87$	
AF-FFF/MALS	$\langle N \rangle_{\text{w}} = 37$	$\langle R_{\text{g}} \rangle_{\text{z}} = 63$	$R_{\text{g}} = 118$
DLS (CONTIN)		$\langle R_{\text{h}} \rangle_{\text{z}} = 58$ (pH < 6)	$R_{\text{h}} = 200-350$
		$\langle R_{\text{h}} \rangle_{\text{z}} = 90$ (pH > 6)	
cryo-TEM	$\langle N \rangle_{\text{n}} = 28$	$\langle R_{\text{core}} \rangle_{\text{n}} = 25$	$\langle R_{\text{core}} \rangle_{\text{n}} \geq 60$
SEM		$\langle R \rangle_{\text{n}} = 25$	$R = 100-250$
SFM		$\langle R \rangle_{\text{n}} = 44$	$R \approx 250$

corresponds to the value for the core (obtained by cryo-TEM), which might indicate that the PMAA corona was destroyed by the electron beam.

(iv) Finally, *what is the structure of the huge particles?* These particles consistently have been observed by all methods, most

strikingly by SEM and SFM. They might be aggregates of supermicelles, but it is difficult to imagine why they should be perfectly spherical. If they were vesicles, they should collapse on the silicon wafer, which is not the case. We speculate that they are multilamellar vesicles, but more experiments, e.g. freeze-fracture TEM, will be needed to clarify this point.

Acknowledgment. The authors acknowledge Reimund Stadler for initiating this project and Paul Bomans for his help during the cryo-TEM measurements. Financial support of this work was given by the *Deutsche Forschungsgemeinschaft* within the “*Schwerpunktprogramm Polyelektrolyte*” (Sta 272/8-2, Mu 896/11-3). We acknowledge support of the SFM and SEM facilities by the SFB 481 (TP Z2) and the BIMF.

JA028982Q